2014 IEEE International Conference on Robotics & Automation (ICRA)
Hong Kong Convention and Exhibition Center
May 31 - June 7, 2014. Hong Kong, China

Experimental Verification of an Approach for Disturbance Estimation and Compensation on a Simulated Biped during Perturbed Stance*

Jie Zhao, Qi Liu, Steffen Schütz, and Karsten Berns

Abstract— **Human shows remarkable skills in reactive balancing control on unknown disturbances while standing and walking. Though current bipedal robots can walk, run and step obstacles, they normally perform in a well-controlled environment. Unexpected perturbations can cause the tumbling of bipedal robots when they possess limited capability of rejecting disturbances. Studies upon neurology and psychophysics of human stance attempt to trace how the human deals with external disturbances. This paper introduces a methodology for disturbances estimation and compensation (DEC) for bipedal robot during standing. Previous psychophysical studies of human self-motion perception indicate that humans estimate and compensate disturbances as follows: firstly, multi-sensory inputs are fused to provide explicit measures and then the estimations of the external disturbances are performed based on them. Then, the estimations are fed into a local feedback control loop, compensating the disturbances. Thus, an approach of disturbance estimation and compensation is developed according to the psychophysical aspects of human. Various experiments, for instance, standing on a rotating plate with varying frequency and amplitudes and continuous external contact forces upon the torso of a bipedal robot, are implemented. Through analyzing and verifying the experimental results on a simulated biped, one can state that the DEC approach successfully serves the bipedal robot during perturbed stance.**

I. INTRODUCTION

While humans easily handle unexpected perturbations, bipedal robots still have to strengthen significantly the capabilities of operating in complex environments. Disturbance rejection and tumbling prevention for bipedal robots are always of highest priority. Otherwise, an unexpected fall can cause harmful damage to the bipedal robot itself and even the peripheral equipment. Detecting how a bipedal system is approaching to falling is yet intriguing due to the nonlinear, underactuated and a hybrid of continuous and discrete dynamics. Present stability approaches for bipedal robots based on zero moment point (ZMP), can be only applied to specific motions or groups of bipedal robots [1]–[3]

Lee *et al*. [4] propose a balancing controller based on compensating linear and angular momentum. The approach suggests that it controls the desired ground reaction force and center of pressure (CoP) at each foot, allowing it to handle different ground geometry. Those aforementioned approaches are based on comparing actual position of CoP or CoM to the desired ones, therefore predefined trajectories of joints are developed in advance.

*This work was funded by the European Commission 7th Framework Program under the project H_2R (no.60069).

All authors are with the Robotics Research Lab, Department of Computer Science, University of Kaiserslautern, 67663 Kaiserslautern, Germany {zhao,schuetz,berns}@cs.uni-kl.de

Recently neurologists [5] and clinicians [6] diagnose balancing problem of human in order to understand the humans' ability of postural control in presence of unexpected disturbances. To detect the principles of the neurological and sensory system for human stance, Fitzpatrick *et al*. [5] express the relationship between ankle torque and angle as a load stiffness. The torque versus angle show that the leg muscles behave elastically during low frequency postural sway. It also states that stabilizing upright posture has been considered to require an integrated reflex response of visual, vestibular and proprioceptive sensory inputs. Brandt [7] finds that an acute failure of vestibular sensory system causes instability and falling, which hints that the vestibular system is part of the human stance control. Consequently, Mergner *et al*. propose a disturbance estimation and compensation [8] approach based on single inverted pendulum model (SIPM) and reconstruct the vestibular system and estimating sensory information of the external disturbances. Hence, the estimations are fed into a local ankle controller to compensate the disturbances.

Hettich *et al*. develop a double inverted pendulum model (DIPM) for human to promote the robustness of postural control [9]. Biomechanical research shows that humans often utilize also the hip joints in addition to the ankle joints to improve their balancing. This paper will introduce two DEC models and their control structure for postural control of human stance that are proposed in [8], [9]. At first, it introduces the fundamental aspects of psychophysical systems of human stance, in which the physical variables, the multisensory inputs and the external disturbances are identified. Based on the psychophysics of human stance, the DEC model and its controller for compensating disturbances are developed for simulated biped. Since a biologically inspired control structure has been applied to a simulated biped, we will address the integration of the DEC method into the existing control structure. As a result of the integration, an estimation of external or self-produced disturbances is suggested and experiments upon a physically simulated biped are presented. Finally, the comparison between experimental results of simulation and human experiments show its applicability and adaptability for the postural control for bipedal robot.

II. BACKGROUND

In human experiments, postural control with almost exclusively the ankle joint is called 'ankle strategy', while additional anticipation of the hip joint is called 'hip strategy'.

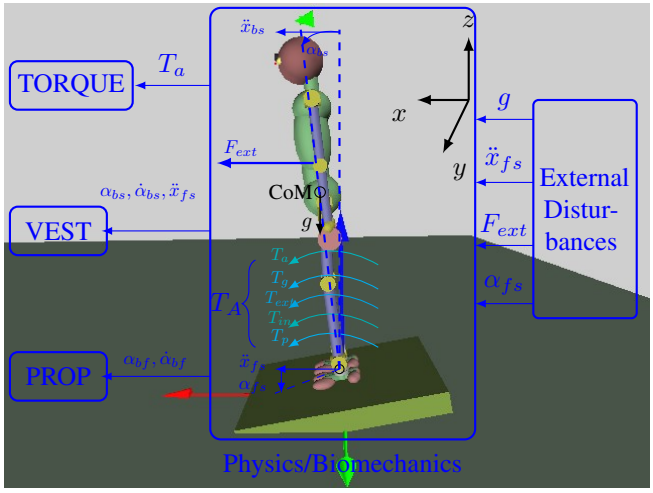

Fig. 1: A SIPM for human stance. It illustrates four different external inputs, the effective ankle torques, the sensor systems and the physical variables measured by sensors. The bs, bf and fs stand respectively for body-space, body-foot and foot-space. The VEST and PROP represent vestibular sensory system and ankle angle proprioception system individually.

A. SIPM

1) Fundamental Physics: Induced gravitational torque tends to turn SIPM over due to its limited stability. Thus, gravity will be considered an external disturbance. With the often studied external disturbances, *i.e.*, tilted surface of support, translation of surface, and imposed forces, they are the four disturbances that will be studied in this paper. Since the sensors and the physical variables they measure play an important role, the fundamental physical inputs shall be introduced in detail.

The four external mechanical disturbances are illustrated in Fig. 1 (torque induced by gravity, g, external force, F_{ext}, ankle angular displacement, α_{fs}, and surface translation with foot-space translational acceleration in sagittal plane, $\ddot{x}_{fs}$) together with their effects on the sensors in the scope of a SIPM. Combined ankle torque T_A is expressed with respect to angular body-space by

$$T_A = J \cdot \ddot{\alpha}_{bs}, \tag{1}$$

where J denotes the body's moment of inertia with respect to the ankle joint and α_{bs} the body-space angle ($\alpha_{bs} = 0°$ for the desired vertical position). In the presence of disturbances, T_A is composed of following components:

$$T_A = T_g + T_{in} + T_{ext} + T_p + T_a, \tag{2}$$

where T_g is the gravitational torque, T_{in} the inertial torque, T_{ext} the external torque, T_p the passive joint torque (induced from internal stiffness and damping) and T_a the exerted torque at ankle joints. The computation of them are given in following way:

$$\begin{aligned} T_g &= m \cdot g \cdot h \cdot \sin(\alpha_{bs}) && (3)\\ T_{in} &= -m \cdot h \cdot \ddot{x}_{fs} \cdot \cos(\alpha_{bs}) && (4)\\ T_{ext} &= F_{ext} \cdot h^{'} \cos(\alpha_{bs}) && (5)\\ T_p &= \mathrm{sgn}\,(\alpha_{bf}) \cdot K_s \cdot {\alpha_{bf}}^2 - K_d \cdot \dot{\alpha}_{bf}, && (6) \end{aligned}$$

where m is the mass of CoM, h is the vertical distance from ankle joint to CoM, $h^{'}$ denotes the height of force impact above the ankle. Concerning the passive joint torque as shown in Eq. (6), K_s and K_d indicate a non-linear spring and damper constant at each joint , and α_{bf} and $\dot{\alpha}_{bf}$ represent the position and velocity of ankle joint respectively.

2) Multisensory Systems: Fig. 1 also gives the main physical variables that are measured by the following three sensor systems:

1) *Ankle torque sensor* (TORQUE). The ankle torque can be measured by a Golgi tendon organ.
2) *Vestibular system* (VEST). It provides mainly the measures for global stability, *e.g.*, vertical body-space angle α_{bs} and its velocity $\dot{\alpha}_{bs}$ and a measure for foot-space translational acceleration $\ddot{x}_{fs}$.
3) *Ankle angle proprioception* (PROP). It offers measurements of the position α_{bf} and velocity $\dot{\alpha}_{bf}$ of ankle joint respectively.

Clinical and experimental evidence suggest that sensors do not work as separate devices, but act as fusion systems of the signals from various sensors. For disturbance estimation and compensation, those sensor systems (vestibular, ankle angle, ankle torque) emerge to be instrumental.

B. DIPM

The mechanical model of DIP is depicted in Figure 2, in which the body is separated into two parts termed as the upper trunk segment(including head and trunk) and the lower trunk segment(including legs and feet). Several vestibular

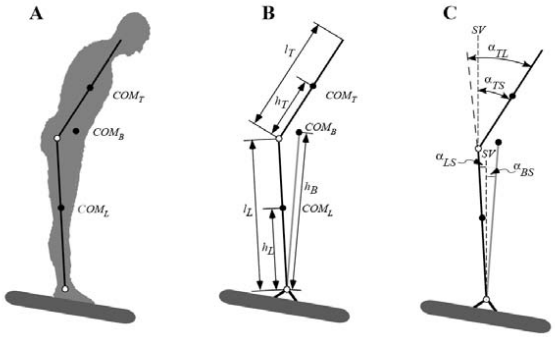

Fig. 2: Human DIPM, parameters of segments, CoM heights and angles [9].

and proprioceptive sensory signals, such as trunk-space angle α_{TS}, trunk-leg angle α_{TL} and leg-space angle α_{LS}, are instrumental for controlling the movement of the upper and lower segments. A body-space angle α_{BS} is defined as the

angular excursion between the line from the body's CoM to the ankle joint and the vertical space. The detailed calculation for ankle joint torque T_A and hip joint torque T_H can be referred to [9].

C. Posture Control for Stance

Generally, postural control is considered to be a complex skill rather than the result of only local reflex action [10]. As the situations of stance can be distinguished into quiet standing and standing under disturbances, we will introduce the posture control for them in the following.

1) Undisturbed Stance: Winter et al. propose a simple control scheme for quiet standing where the ankle muscles act as springs [11], [12]. This introduces a stiffness control for balancing that can react mechanically and quickly. Luksch [13] introduces a stiffness controller for standing in unstructured terrain. It firstly configures the joints to a low stiffness and sets the current joint position as the target angle of joint. As the foot gradually contacts the ground, the stiffness and the target angle are passively adapted to the situation. After the posture is stabilized and a sufficiently quiet stance is achieved, the target pose can be optimized consequently.

2) Disturbed Stance: Maurer *et al*. [14] observe that disturbance compensation increases with ascending disturbance magnitude and mention that aforementioned three sensory systems can predict the system disturbances. Mergner [15] concludes that reactive human stance control can be described as a model of a feedback loop in which the multisensory systems, the disturbance estimation units and a control mechanism present. Hettich [9] *et al*. extend the control for SIPM to the DIPM afterwards.

III. DEC MODELS AND THE CONTROLLERS

To reject the unforeseen external disturbances of varying amplitude and frequency, sensory information have to be integrated into the control system. The proposed DEC control consists of two main blocks, *i. e.* sensory signals and online sensory disturbance estimation. The block of sensory signals is derived from psychophysical evidence. It implies that signals from different sensors are fused in order to provide measures of physical variables. The second block origins from psychophysical studies, which imply that sensor signals do not directly conscious human perceptions. Therefore, sensor signals are fused with each other and with cognition to yield estimates of the external disturbances. The computations concerning sensory disturbance estimations are described in the following.

A. SIPM

1) Estimate of Foot-Support Space Rotation $\hat{\alpha}_{fs}$: During support surface rotation about the ankle joint axes, the compensation of rotation is assumed to fulfill through an estimation of the rotation, $\hat{\alpha}_{fs}$. The estimate $\hat{\alpha}_{fs}$ is obtained from $\dot{\alpha}_{bs}$ and $\dot{\alpha}_{bf}$, which are aggregated to generate an estimate of foot-space velocity $\dot{\alpha}_{fs}$ in the form of

$$\hat{\dot{\alpha}}_{fs} = \dot{\alpha}_{bs} - \dot{\alpha}_{bf}. \tag{7}$$

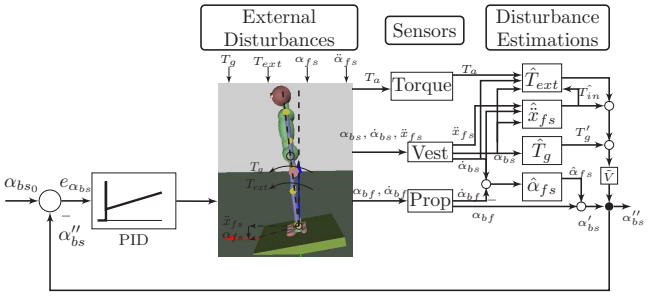

Fig. 3: Disturbance estimation and compensation model of human postural control in standing. It estimates online the external disturbances based on sensory inputs. Afterwards, it feeds the estimated variables into the a proprioceptive feedback loop for disturbance rejection. In the box $\tilde{V}$, it converts an estimated torque T, which is the sum of estimation of all torques induced by disturbances, into the body-space angle equivalent ($\arcsin(T/mgh)$).

Further processing consists of a velocity threshold and a mathematical integration. It feeds the estimate $\hat{\alpha}_{fs}$ into the proprioceptive α_{bf} loop, producing a body-space variable

$$\alpha'_{bs} = \hat{\alpha}_{fs} + \alpha_{bf}. \tag{8}$$

2) Estimate of Gravitational Torque $\hat{T}_g$: Feeding a vestibular body-space angle α_{bs} into the estimate $\hat{T}_g$, it yields an internal gravitational torque T'_g:

$$T'_g = m \cdot g \cdot h \cdot \sin(\alpha_{bs}) \tag{9}$$

(compare Eq. (3)), where $m \cdot g \cdot h$ is an identified quantity.

3) Estimate of Foot-Space Translational Acceleration $\hat{\ddot{x}}_{fs}$: This estimate has calculated the $\hat{\ddot{x}}_{fs}$ from two vestibular signals in which

$$\hat{\ddot{x}}_{fs} = \ddot{x}_{fs} \cdot \cos(\alpha_{bs}) + \ddot{\alpha}_{bs} \cdot d - \frac{d(\dot{\alpha}_{bs})}{dt} \cdot d, \tag{10}$$

where $\ddot{\alpha}_{bs} \cdot d$ represents the tangential acceleration during eccentric rotation with d denoting the distance of the vestibular sensor in the head from the ankle and $\dot{\alpha}_{bs}$ is the measure for angular velocity at the head with respect to the ankle joint. Besides, an internal evoked inertial torque T'_{in} is derived from $\hat{\ddot{x}}_{fs}$ and the α_{bs} through:

$$T'_{in} = -\hat{\ddot{x}}_{fs} \cdot m \cdot h \cdot \cos(\alpha_{bs}). \tag{11}$$

4) Estimate of External Torque $\hat{T}_{ext}$: The estimate $\hat{T}_{ext}$, which results from the external forces, is obtained from the ankle torque sensor, the vestibular and the ankle proprioceptive sensor. The calculation is as:

$$T'_{ext} = T'_A - T'_g - T'_{in} - T'_p - T'_a \tag{12}$$

where T'_g and T'_{in} are given respectively in Eq. (9) and (11), T'_a the measured ankle torque, T'_A and T'_p can be calculated by comparing to Eq. (1) and (6) individually.

5) Controller in the Feedback Loop: As mentioned above, the values from DEC model are fed into a feedback loop for disturbance rejections. A typical PID (proportional-integral-derivative) controller is applied to this system. The transfer function of the PID controller $T_c(s)$ is in the form of

$$T_c(s) = k_p + k_i \cdot \frac{1}{s} + k_d \cdot s. \tag{13}$$

In order to settle the configuration of T_c, we start from the parameter k_p. Firstly, only a proportional controller is inserted into the feedback loop. Given a slow rotation of the plate as disturbance, the k_p is configured if it can just stabilize the biped in presence of disturbance. Then the frequency of rotation increases gradually to 2 Hz, thus a k_d is inserted in order to follow the dynamics of the rotating plate. At last, by decreasing the frequency and increasing the amplitude of the rotation, the k_i is designed. In our experiments, those parameters are set as $k_p = 8$, $k_i = 0.1$, and $k_d = 6$ respectively.

B. DIPM

As seen in Fig. 2, the control for DIPM requires the torques of both the ankle and hip joints.

The control of the upper trunk inherits the control method of a SIPM, in which the inter-link coupling effects are treated as external disturbances where other estimation for disturbances can be referred to Sec. III-A.

The ankle joint has to balance the whole body though in *hip strategy*. The basic idea of ankle control is again to simplify the human body as a SIPM, which means that it controls the ankle joints through the body-space angle signal α_{bs}. Thus, the whole-body CoM, CoM_B, is always controlled in a stable range by generating torques at ankle joints. At last,

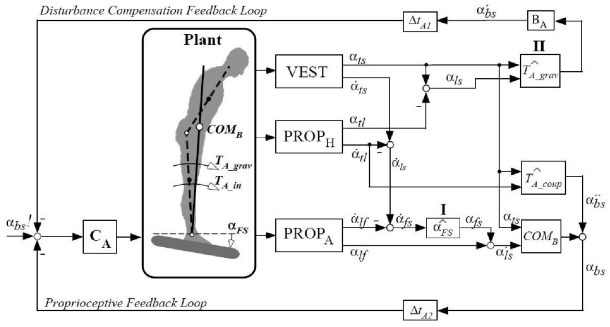

Fig. 4: Ankle control block diagram for DIPM [9].

the hip and ankle control model are fused in a way that the vestibular sensors and proprioceptive measurements for hip are shared [9].

IV. A BIOLOGICALLY CONTROLLED BIPED

A. Biped Setup

A bipedal robot model, which is based on human gait analysis associating with the most relevant joints for walking, is developed as the simulation subject. The overall system amounts to 21 degrees of freedom, and the robot's height adds up to 1.8 m and it weighs 76 kg.

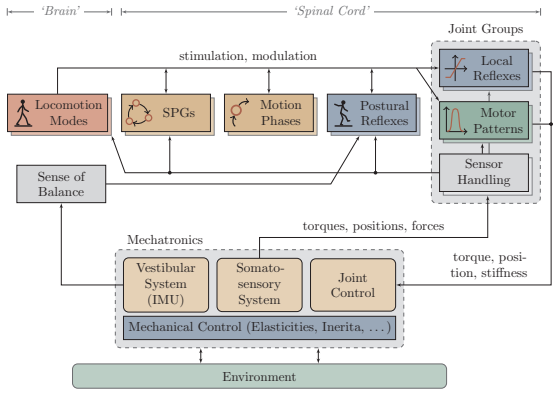

Fig. 5: Hierarchical organization of control units [13].

B. Control Structure

A biologically motivated control method emerges as a transfer of key features found in biomechanics and biology of human walking control to biomimetic robotics [13]. Fig. 5 illustrates the hierarchical layout defined by the flow of stimulation, inhibition, and modulation between six classes of control units. *Locomotion modes* are located at the highest layer and stand for the class of locomotion *e. g.* walking or standing. They stimulate *spinal pattern generators* (SPG), which are state machine-like units. *Motion phases* offer synchronized stimulation of control commands. Feed-forward control is issued by *motor patterns* in the shape of local torque profiles. Feedback control is performed by local and postural reflexes: *local reflexes* only affect spatially related joints based on signals of local sensors. *Postural reflexes* require global sensor information, *e. g.* body orientation, acceleration and etc to control the global stability.

V. INTEGRATION OF DEC MODEL INTO BIOLOGICAL CONTROL STRUCTURE

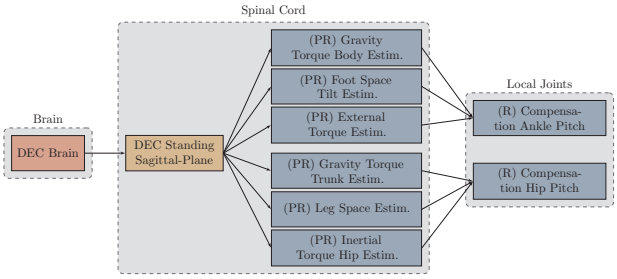

Fig. 6: The integration of DEC model into the biological control structure.

Since the current control structure is hierarchically organized and flow of stimulation, inhibition and modulation can be transferred among layers, the DEC model has to be integrated in a way that it extends the functionality of the current control structure. The integration of DEC into the current control structure is described in the following.

Firstly, in DEC model local sensory signals feed into central sensor processing units. This function can be imple-

mented by constructing a control unit in an upper layer, *i. e. Locomotion Modes*. The control block detects the feet load to check for full foot contact as well as the imposed forces. If a full contact is present and/or an imposed force is detected, a stimulation flows into lower layer *i. e. SPG*. A series of control units are developed in *SPG* that process and fuse multisensory signals as shown in Fig. 6. Then the estimations of external disturbances flow into the local proprioceptive feedback loop. At last, the proprioceptive ankle controllers, which are developed as the lowest layer *i. e. local reflexes*, receive the estimations from *SPG* and compute the torques for ankle joints.

VI. EXPERIMENTAL RESULTS

To verify the proposed control methods and their integration, the support surface tilt is applied as the first disturbance. We apply the sinusoidal rotation of the support surface with the frequency at 3 Hz and the amplitude up to $\pm 6\,^\circ$. Afterwards, an $\pm 4^\circ$ peak-to-peak pseudo-random sequence signals is used. Those experiments data will be compared to the data of human experiments to validate the proposed control method for bipedal robots. The detailed experimental configurations are given in the following.

A. Periodic Rotation of Support Surface

The first experiment configuration applies a periodical rotation on the support surface at the frequency of 3 Hz with an amplitude of up to $\pm 2\,^\circ$ as shown in Fig. 7. This disturbance can be handled by the robot within the *ankle strategy*, thus only the ankle control is introduced here. Due

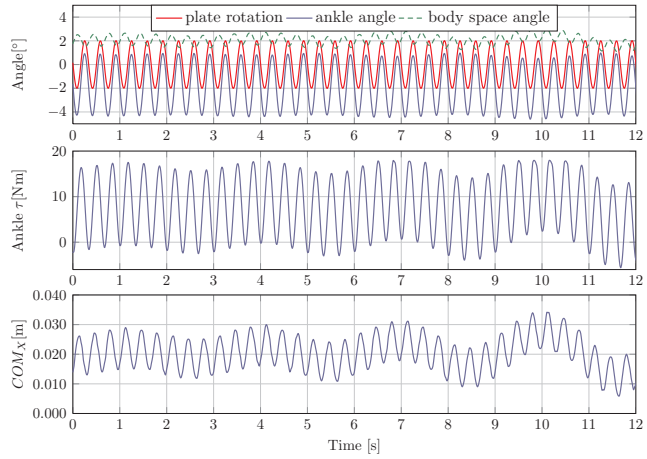

Fig. 7: The experimental results of a biped standing on a periodically rotating plate at the frequency of 3.0 Hz and with the amplitude up to $\pm 2\,^\circ$. The plate rotation is shown in red, where ankle angle α_{bf} is in blue and the body space angle α_{bs} is profiled in dashed green line. The yielded torque T_a at ankle joint and the CoM are illustrated in the second and third row respectively. The experimental data derive from average of both ankle joints in 20 individual tests.

to an offset of the angle at ankle joint, a small minus shift of the peak value of the ankle angle α_{bf} can be observed. This results in a forward tilt of the biped in still standing. Hence, the body space angle α_{bs} tends to have small positive offset because of the forward tilted posture. Given the fact that positive torques at ankle joint tend to plantar-flex the foot and the negative ones to dorsi-flex the foot, the actual torques at ankle joint demonstrate an opposite shape compared to the angle of ankle joint. The position of CoM, denoting the center of mass of this inverted pendulum model, demonstrates a similar periodical course as the torque.

An obvious variation is that the ankle joints have in most time a negative degree and the values of ankle torque and the CoM are positive consequently. Except for the reason mentioned above, another one is that the plate tilts at a relatively high frequency and the estimated body-space angle $\hat{\alpha}_{bs}$ as well as the generated torques at ankle joints can not be calculated in time. The same behavior can be also found in human as shown in Fig. 8. The subject keeps the body along with the inclined platform and after a while shows a slow compensation pf the tilt. This behavior from both the simulation and human experiments indicates the applicability of the proposed control method on robots.

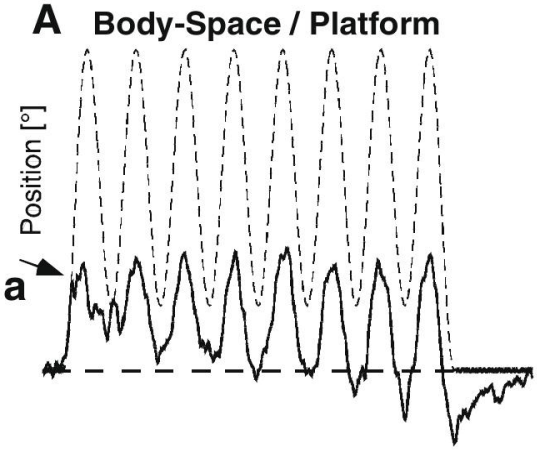

Fig. 8: The experimental results of human standing on a quickly rotating platform [8]. The dashed and solid lines respectively mean the rotation of platform and the ankle angle.

B. Aperiodic Rotation of Support Surface

We have shown experimentally that the DEC works well for bipedal stance in presence of a periodic tilted plate. To check its applicability for aperiodic rotation of the support surface, the following experiment will be applied. The rotation velocity of the plate can not be changed abruptly, otherwise it causes either the toe or heels to leave the plate. In Fig. 9, a random offset of $\pm 0.2\,^\circ$ on a sinusoidal waveform is applied to the biped. Though the ankle joint angle α_{bf} has always a small offset compared to the rotation of the plate, it nearly follows the rotation of the plate. The position of CoM denotes that the robot tilt in a small range compared to its primary position though the random offset exists. These results indicate that the DEC model can also adapt to a random rotation of the plate.

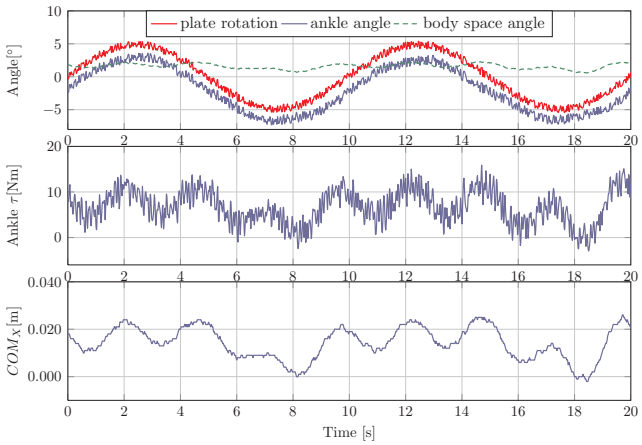

Fig. 9: The experimental results of a biped standing on an aperiodic rotating plate with the amplitude up to $\pm 5\,^\circ$ and the random offset up to $\pm 0.2\,^\circ$.

C. Aperiodic Rotation of Support Surface with Hip Strategy

The *ankle strategy* has been already studied thoroughly, but the *hip strategy* has also to be studied in simulation and the results shall be compared to those in human experiments. In this test, the tilted support surface as disturbance stimulus is applied as shown in Fig. 10. A $\pm 4^\circ$ pseudo-random sequence stimulates the rotation of the platform. One can notice that the body-space angle has a small excursion due to the CoM position as mentioned before.

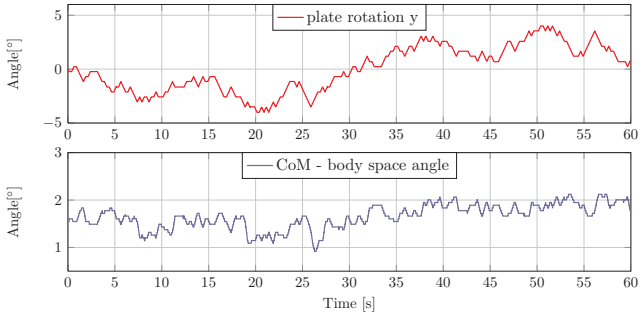

Fig. 10: The pseudo-random tilted platform and the course of CoM of simulated biped.

Six healthy young subjects were standing with closed eyes and presented with the same pseudo-random tilted platform as given in Fig. 10. Average of the last five of six stimulus repetitions of one trial is illustrated in Fig. 11. Comparing the CoM trajectories in Fig. 10 to Fig. 11, it is obviously showing the resemble characteristics.

VII. CONCLUSION AND FUTURE WORK

We have introduced the disturbance estimation and compensation methods for bipedal standing based on biomechanical research. It suggests that multisensory systems in human provide the signals to the information processing centers. Based on the actual signals, a group of variables for disturbance estimations are yielded and feed into a feedback control loop. Afterwards, a biologically inspired

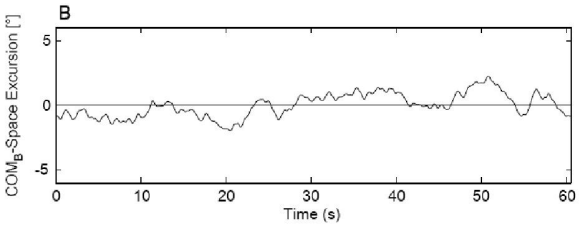

Fig. 11: The course of CoM of a subject [9].

control structure for a biped is suggested and a seamless integration of the proposed DEC into this control structure is developed. At last, varying situations of disturbances, *e. g.*, periodic and aperiodic rotation of the plate are applied as the disturbance stimuli. Experimental results show that DEC works successfully on those situations. Regarding the future work, lateral disturbances will be taken into consideration and an omni-directional rotation of the plate will be tested. Thus, it is required to extend the DEC model to the frontal plane of the biped. To overcome additional challenges, *e. g.* quicker and larger rotation of the plate, more powerful imposed forces and translational platform, it is expected to implement the DEC model at the knee and arm joints, too.

REFERENCES

[1] S.-H. Hyon and G. Cheng, "Disturbance rejection for biped humanoids," in *Robotics and Automation, 2007 IEEE International Conference on*. IEEE, 2007, pp. 2668–2675.

[2] V. Prahlad, G. Dip, and C. Meng-Hwee, "Disturbance rejection by online zmp compensation," *Robotica*, vol. 26, no. 1, p. 9, 2008.

[3] D. G. Hobbelen and M. Wisse, "A disturbance rejection measure for limit cycle walkers: The gait sensitivity norm," *Robotics, IEEE Transactions on*, vol. 23, no. 6, pp. 1213–1224, 2007.

[4] S.-H. Lee and A. Goswami, "Ground reaction force control at each foot: A momentum-based humanoid balance controller for non-level and non-stationary ground," in *Intelligent Robots and Systems (IROS), 2010 IEEE/RSJ International Conference on*. IEEE, 2010, pp. 3157–3162.

[5] R. Fitzpatrick, J. Taylor, and D. McCloskey, "Ankle stiffness of standing humans in response to imperceptible perturbation: Reflex and task-dependent components," *Journal of Physiology - London*, pp. 533–547, 1992.

[6] A. M. Bronstein, T. Brandt, M. H. Woollacott, and J. G. Nutt, *Clinical disorders of balance, posture and gait*. Arnold, 2004.

[7] T. Brandt, *Vertigo: its multisensory syndromes*. Springer, 2003.

[8] T. Mergner, G. Schweigart, and L. Fennell, "Vestibular humanoid postural control," *Journal of Physiology - Paris*, vol. 103, pp. 178 – 194, 2009.

[9] G. Hettich, L. Fennell, and T. Mergner, "Double inverted pendulum model of reactive human stance control," in *Multibody Dynamics Conference 2011*, 2011.

[10] F. B. Horak, "Postural orientation and equilibrium: what do we need to know about neural control of balance to prevent falls?" *Age and Ageing*, vol. 35-S2, pp. ii7–ii11, 2006.

[11] D. Winter, A. Patla, F. Prince, M. Ishac, and K. Gielo-Perczak, "Stiffness control of balance in quiet standing," *Journal of Neurophysiology*, vol. 80, no. 3, pp. 1211–1221, 1998.

[12] D. Winter, A. Patla, S. Rietdyk, and M. Ishac, "Ankle muscle stiffness in the control of balance during quiet standing," *Journal of Neurophysiology*, vol. 85, no. 6, pp. 2630–2633, 2001.

[13] T. Luksch, "Human-like control of dynamically walking bipedal robots," Ph.D. dissertation, University of Kaiserslautern, October 2009.

[14] C. Maurer, T. Mergner, and R. Peterka, "Multisensory control of human upright stance," *Experimental Brain Research*, vol. 171, no. 2, pp. 231–250, 2006.

[15] T. Mergner, "A neurological view on reactive human stance control," *Annual Reviews in Control*, vol. 34, no. 2, pp. 177 – 198, 2010.